Agricultural and Forest Meteorology 173 (2013) 28–39

Contents lists available at SciVerse ScienceDirect

Agricultural and Forest Meteorology

journal homepage: www.elsevier.com/locate/agrformet

Development of a two-leaf light use efficiency model for improving the calculation of terrestrial gross primary productivity

Mingzhu He[a,b], Weimin Ju[a,b,*], Yanlian Zhou[a,c], Jingming Chen[a,b], Honglin He[d], Shaoqiang Wang[d], Huimin Wang[d], Dexin Guan[e], Junhua Yan[f], Yingnian Li[g], Yanbin Hao[h], Fenghua Zhao[d]

[a] Jiangsu Provincial Key Laboratory of Geographic Information Science and Technology, Nanjing University, Nanjing, 210093, China
[b] International Institute for Earth System Sciences, Nanjing University, Nanjing, 210093, China
[c] School of Geographic and Oceanographic Sciences, Nanjing University, Nanjing, 210093, China
[d] Institute of Geographic Sciences and Natural Resources Research, Chinese Academy of Sciences, Beijing, 100101, China
[e] Institute of Applied Ecology, Chinese Academy of Sciences, Shenyang, 110016, China
[f] South China Botanical Garden, Chinese Academy of Sciences, Guangzhou, 510650, China
[g] Northwest Institute of Plateau Biology, Chinese Academy of Sciences, Xining, 810008, China
[h] Graduate University of Chinese Academy of Sciences, Beijing, 100049, China

ARTICLE INFO

Article history:
Received 20 July 2012
Received in revised form 8 November 2012
Accepted 10 January 2013

Keywords:
Gross primary productivity
Two-leaf light use efficiency (TL-LUE) model
MOD17 algorithm
Sunlit and shaded leaves

ABSTRACT

Gross primary productivity (GPP) is a key component of land–atmospheric carbon exchange. Reliable calculation of regional/global GPP is crucial for understanding the response of terrestrial ecosystems to climate change and human activity. In recent years, many light use efficiency (LUE) models driven by remote sensing data have been developed for calculating GPP at various spatial and temporal scales. However, some studies show that GPP calculated by LUE models was biased by different degrees depending on sky clearness conditions.

In this study, a two-leaf light use efficiency (TL-LUE) model is developed based on the MOD17 algorithm to improve the calculation of GPP. This TL-LUE model separates the canopy into sunlit and shaded leaf groups and calculates GPP separately for them with different maximum light use efficiencies. Different algorithms are developed to calculate the absorbed photosynthetically active radiation for these two groups. GPP measured at 6 typical ecosystems in China was used to calibrate and validate the model. The results show that with the calibration using tower measurements of GPP, the MOD17 algorithm was able to capture the variations of measured GPP in different seasons and sites. But it tends to understate and overestimate GPP under the conditions of low and high sky clearness, respectively. The new TL-LUE model outperforms the MOD17 algorithm in reproducing measured GPP at daily and 8-day scales, especially at forest sites. The calibrated LUE of shaded leaves is 2.5–3.8 times larger than that of sunlit leaves. The newly developed TL-LUE model shows lower sensitivity to sky conditions than the MOD17 algorithm. This study demonstrates the potential of the TL-LUE model in improving GPP calculation due to proper description of differences in the LUE of sunlit and shaded leaves and in the transfer of direct and diffuse light beams within the canopy.

1. Introduction

The carbon cycle of terrestrial ecosystems is interactively linked with the global climate system at various temporal and spatial scales and has been a focus of global change studies in recent decades. Gross primary productivity (GPP), the integral of photosynthesis by all leaves (Lieth, 1973), is a key component of the terrestrial carbon cycle (Field et al., 1998; Yang et al., 2007; Gao and Liu, 2008). Quantitative estimates of GPP at global/regional scales are necessary for understanding the response of terrestrial ecosystems to the increases in atmospheric CO_2 and temperature and to various natural and human-induced disturbances (Metz et al., 2006).

In recent decades, a variety of models have been developed for calculating regional/global GPP, embracing process-based ecological models and remote sensing driven light use efficiency (LUE) models. Widely used LUE models, such as CASA (Potter et al., 1993), MOD17 algorithm (Running et al., 2000), VPM (Xiao et al., 2004a,b), EC-LUE (Yuan et al., 2007), commonly calculate GPP or NPP (net primary productivity) as the product of absorbed photosynthetically active radiation (APAR) and LUE, which is downscaled from

* Corresponding author at: Jiangsu Provincial Key Laboratory of Geographic Information Science and Technology, Nanjing University, Nanjing, 210093, China.
E-mail address: juweimin@nju.edu.cn (W. Ju).

0168-1923/$ – see front matter © 2013 Elsevier B.V. All rights reserved.
http://dx.doi.org/10.1016/j.agrformet.2013.01.003

the maximum by the scalars of temperature, soil water content, and atmospheric water vapor pressure deficit. The differences in various LUE models mainly exist in the ways of calculating APAR and these scalars and in the determination of maximum LUE. The MOD17 algorithm, which is currently used to produce the global GPP product (MOD17A2) in near real time, calculates APAR on the basis of Beer's law (Jarvis and Leverenz, 1983) and remotely sensed leaf area index (LAI) and integrates the effects of minimum temperature and water vapor deficit on GPP.

Recent validations using tower-based GPP show that there are some uncertainties in MODIS GPP related to inaccuracy of input meteorological data (Baldocchi et al., 2001; Turner et al., 2003; Zhao et al., 2005, 2006; Heinsch et al., 2006; Nightingale et al., 2007), remotely sensed LAI (Wang et al., 2004; Hill et al., 2006; Zhang et al., 2008), and the underestimation of the maximum light use efficiency (ε_{max}) (Running et al., 2004; Zhang et al., 2008). In addition, the assumption that GPP linearly increases with APAR in LUE models, such as the MOD17 algorithm, has been recently proved to be sometimes questionable (Zhang et al., 2011; Propastin et al., 2012). Many studies indicated that GPP and LUE are affected by both the quantity and composition of the incoming solar radiation. With a given value of total incoming radiation, LUE of entire canopy will increase with the increasing fraction of diffuse radiation that results in an increase in the canopy fraction that is receiving illumination without photo-saturation (Roderick et al., 2001; Mercado et al., 2009; Oliphant et al., 2011; Zhang et al., 2011). A recent study conducted by Propastin et al. (2012) found that for a tropical rainforest in Sulawesi, Indonesia, GPP of the MOD17A2 product was underestimated during phases of low photosynthesis production due to the underestimation of MODIS *f*PAR (fraction of photosynthetically active radiation) and was overestimated during phases with clear sky conditions due to the fact that the MOD17A2 algorithm ignores the saturation effect of canopy photosynthesis under the conditions of high incoming solar radiation.

Sunlit leaves within the canopy can simultaneously absorb direct and diffuse radiation. Under clear sky conditions, these leaves are often light saturated, resulting in low LUE. In contrast, shaded leaves suffer from a lower exposure to incoming radiation. Their photosynthesis is limited by low APAR. Under cloudy or aerosol-laden skies, incoming radiation is more diffuse and more uniformly distributed in the canopy with a smaller faction of the canopy that is light saturated. As a result, canopy photosynthesis tends to be significantly more light-use efficient under diffuse sunlight than under direct sunlight conditions (Roderick et al., 2001; Gu et al., 2002, 2003; Niyogi et al., 2004; Misson et al., 2005; Urban et al., 2007; Mercado et al., 2009; Sun and Zhou, 2010; Oliphant et al., 2011;).

In order to quantify the effect of changes in the quality of incoming radiation on GPP, models need to stratify the canopy into sunlit and shaded leaves and consider the differences in the transfer of direct and diffuse beams within the canopy (Mercado et al., 2009). Many ecological models and land surface process models recently separate canopy into shaded and sunlit leaves for which APAR and GPP are individually calculated (Norman, 1993; De Pury and Farquhar, 1997; Wang and Lenuing, 1998; Chen et al., 1999). However, all LUE models, including the MOD17 algorithm, currently treat the whole canopy as a big extended leaf and ignore the difference in APAR and LUE of leaves at different locations within the canopy. These simplifications would induce systematic errors in calculated GPP (De Pury and Farquhar, 1997; Wang and Lenuing, 1998; Chen et al., 1999).

The aims of this study are: (1) to develop a light use efficiency model (TL-LUE) with sunlit and shaded leaf separation based on the MOD17 algorithm, (2) to prove that the TL-LUE model outperforms the MOD17 algorithm in calculating GPP, and (3) to test the hypothesis that LUE of sunlit and shaded leaves differs significantly. GPP measured at 6 typical sites (including three forest sites, two grassland sites, and one cropland site) using the eddy covariance technique was used as benchmarks for calibrating maximum LUE and valuating the performance of the TL-LUE model. China is in the east monsoon area of Eurasia, and has diverse climates and ecosystems. Terrestrial ecosystems play an important role in the global carbon cycle (Piao et al., 2005; Wang et al., 2007) and outcomes of this study can offer valuable references for calculating GPP in other regions.

2. Data and method

2.1. Data

2.1.1. Flux data

GPP measured at 6 typical sites across China was used for model calibration and validation in this study (Fig. 1), including the Changbai Mountain pine and broadleaf mixed forest site (CBS) (Zhang et al., 2006a; Yu et al., 2006), Qianyanzhou planted coniferous forest site (QYZ) (Zhang et al., 2006a; Yu et al., 2006), Dinghushan South Subtropical evergreen broadleaved forest site (DHS) (Zhang et al., 2006a; Yu et al., 2006), Yucheng warmer temperate dry farming cropland (YC) (Zhang et al., 2008; Li et al., 2006), Haibei alpine meadow (HB) (Zhang et al., 2008; Li, 2006), and Xinlinhot grassland in Inner Mongolia (XLHT) (Liu et al., 2011). The main information on vegetation and climate of these sites is summarized in Table 1.

Daily and 8-day GPP data are derived from the net ecosystem productivity (NEP) measured every 30-min using the eddy covariance technique. GPP was calculated from the measured NEP, which was processed using the same method as Zhang et al. (2011). A model based on the Lloyd–Taylor equation (Lloyd and Taylor, 1994) for calculating ecosystem respiration (Re) was firstly fitted using the nighttime NEP data under turbulent conditions (Fu et al., 2006a,b; Yu et al., 2008), i.e.

$$\mathrm{NEP} = \mathrm{Re} = R_{\mathrm{ref}} \mathrm{e}^{E_0 (1/(T_{\mathrm{ref}} - T_0) - 1/(T - T_0))} \quad (1)$$

where R_{ref} represents the ecosystem respiration rate at a reference temperature (T_{ref}, 10 °C); E_0 is the parameter that determines the temperature sensitivity of ecosystem respiration, and T_0 is a constant and set as −46.02 °C; and T is the air temperature or soil temperature (°C).

Eq. (1) was employed in conjunction with measured NEP to calculate GPP, i.e.

$$\mathrm{GPP} = \mathrm{Re} + \mathrm{NEP} \quad (2)$$

In order to reduce the influences of the uncertainties in meteorological data on GPP calculation, the in situ measured meteorological data, including PAR, air temperature (T_a), and vapor pressure deficit (VPD), are used to drive the model. The daily meteorological data are obtained by averaging or minimizing the original 30-min data.

Data measured at CBS, QYZ, DHS, YC, and HB in 2003 and at XLHT in 2004 were used to calibrate model parameters. Data measured at CBS, QYZ, DHS, YC, and HB in 2004 and at XLHT in 2007 were used for model validation.

2.1.2. MODIS data

The MOD15A2 and MOD17A2 products were used here. MOD17A2 is the GPP product and MOD15A2 is the LAI and *f*PAR products. They are all the 8-day composites and were downloaded from the website of Land Processes-Distributed Active Archive Center (LPDAAC) (http://lpdacc.usgs.gov/get_data). MOD17A2 GPP and MOD15A2 LAI in a 2-year period from January 1, 2003 to December 31, 2004 were used for the CBS, QYZ, DHS, YC, and HB sites, and those in a 2-year period from January 1, 2004 to December 31, 2004 and from January 1, 2007 to December 31, 2007 were

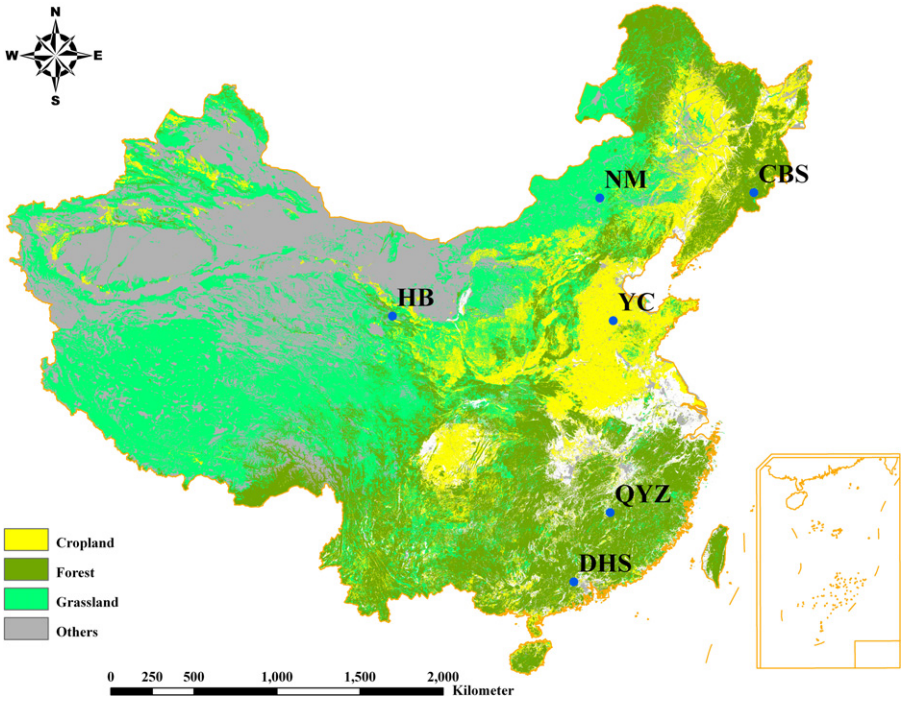

Fig. 1. Distribution of the 6 sites in China at which measured GPP was used for calibrating and validating the TL-LUE model developed in this study. The background is the GLC2000 land cover map.

used for the XLHT site. Both the MODIS GPP and LAI products have a spatial resolution of 1 km. The projection of these data is Sinusoidal, and MRT (MODIS Reprojection Tools) was used to reproject them into an UTM/WGS 84 projection. Because of residual cloud contamination, the MODIS LAI product has some unrealistically abrupt short-term fluctuations, and the locally adjusted cubic-spline capping (LACC) method (Chen et al., 2006) was used to smooth MODIS LAI. The smoothed LAI series were then input into the MOD17 algorithm and the TL-LUE model for calculating *f*PAR.

2.2. Method

2.2.1. The MOD17 algorithm

The MOD17 algorithm is based on the radiation conversion efficiency concept of Monteith (1972). GPP is calculated as (Running et al., 2000):

$$\mathrm{GPP} = \varepsilon_{\max} \times f(\mathrm{VPD}) \times g(T_a) \times \mathrm{PAR} \times f\mathrm{PAR} \quad (3)$$

where *f*PAR is the fraction of PAR absorbed by the canopy and calculated as:

$$f\mathrm{PAR} = 1 - \mathrm{e}^{-k \times \mathrm{LAI}} \quad (4)$$

where k is the light extinction coefficient and set as 0.5; LAI is the green leaf area index of the whole canopy.

In Eq. (3), $\varepsilon_{\max}$ is the maximum LUE and changes with vegetation types (Table 2). $f(\mathrm{VPD})$ and $g(T_a)$ are the scalars of VPD and the minimum air temperature (T_a) used to downscale $\varepsilon_{\max}$ to the actual. They are calculated as:

$$f(\mathrm{VPD}) = \begin{cases} 0 & \mathrm{VPD} \geq \mathrm{VPD}_{\max} \\ \dfrac{\mathrm{VPD}_{\max} - \mathrm{VPD}}{\mathrm{VPD}_{\max} - \mathrm{VPD}_{\min}} & \mathrm{VPD}_{\min} < \mathrm{VPD} < \mathrm{VPD}_{\max} \\ 1 & \mathrm{VPD} \leq \mathrm{VPD}_{\min} \end{cases} \quad (5)$$

$$g(T_a) = \begin{cases} 0 & T_a \leq T_{\min} \\ \dfrac{T_a - T_{\min}}{T_{\max} - T_{\min}} & T_{\min} < T_a < T_{\max} \\ 1 & T_a \geq T_{\max} \end{cases} \quad (6)$$

Table 1
Summary of climate and vegetation characteristics of the 6 tower sites.

Sites	Changbaishan	Qianyanzhou	Dinghushan	Yucheng	Haibei	Xinlinhot
Lat/Lon	42°24′N 128°06′E	26°45′N 115°04′E	23°10′N 112°32′E	36°57′N 116°36′E	37°40′N 101°20′E	43°33′N 116°40′E
Climate type	Temperate continental climate influenced by monsoon	Sub-tropical monsoon climate	The monsoon humid climate of torrid zone of south Asia	Semi-humid and monsoon climate	Plateau continental climate	Temperate semiarid continental climate
Annual mean precipitation (mm)	600–900	1489	1956	582	580	350–450
Annual mean temperature (°C)	3.6	18.6	21	13.1	−1.7	−0.4
Vegetation type	Mixed forest	Evergreen needleleaf forest	Evergreen broadleaf forest	Winter wheat/summer corn	Alpine meadow	Grassland

Table 2
Parameters ε_{max}, VPD_{max}, VPD_{min}, T_{min}, T_{max}, albedo (α) and clumping index (Ω) of different vegetation types.

Vegetation type[a]	ENF	EBF	MF	Grass	Crop
ε_{max} (g C MJ^{-1})	1.008	1.259	1.116	0.604	0.604
T_{max} (°C)	8.31	9.09	8.50	12.02	12.02
T_{min} (°C)	8.00	8.00	8.00	8.00	8.00
VPD_{max} (kpa)	4.10	4.10	4.10	4.10	4.10
VPD_{min} (kpa)	0.93	0.93	0.93	0.93	0.93
α	0.15	0.18	0.17	0.23[c]	0.23[d]
Ω[b]	0.6	0.8	0.7	0.9	0.9

[a] ENF: evergreen needleleaf forest; EBF: evergreen broadleaf forest; MF: mixed forest.
[b] Tang et al. (2007).
[c] Grant et al. (2000).
[d] Singarayer et al. (2009).

where VPD_{max}, VPD_{min}, T_{min}, T_{max} are the parameters dependent on vegetation types (Running et al., 2000) (Table 2).

2.2.2. Development of a two-leaf light use efficiency model

A two-leaf light use efficiency model (TL-LUE) is developed on the basis of the MOD17 algorithm. It separates the canopy into sunlit and shaded leaf groups and calculates GPP for each of them. GPP of the whole canopy is calculated as:

$$GPP = (\varepsilon_{msu} \times APAR_{su} + \varepsilon_{msh} \times APAR_{sh}) \times f(VPD) \times g(T_a) \quad (7)$$

where ε_{msu} and ε_{msh} are the maximum LUE of sunlit and shaded leaves, respectively; $APAR_{su}$ and $APAR_{sh}$ are the PAR absorbed by sunlit and shaded leaves and calculated as:

$$APAR_{sh} = (1-\alpha) \times \left[\frac{PAR_{dif} - PAR_{dif,\,u}}{LAI} + C \right] \times LAI_{sh} \quad (8)$$

$$APAR_{su} = (1-\alpha) \times \left[PAR_{dir} \times \frac{\cos(\beta)}{\cos(\theta)} + \frac{PAR_{dif} - PAR_{dif,u}}{LAI} + C \right] \times LAI_{su} \quad (9)$$

where α is the albedo related to vegetation types (Table 2); PAR_{dif} and PAR_{dir} are the diffuse and direct components of incoming PAR, respectively, and they are calculated using equation 10; $PAR_{dif,u}$ is the diffuse PAR under the canopy and calculated following Chen et al. (1999); ($PAR_{dif} - PAR_{dif,u}$)/LAI represents the diffuse PAR on per unit leaf area within the canopy; C quantifies the contribution of multiple scattering of the total PAR to the diffuse irradiance per unit leaf area within the canopy; β is mean leaf-sun angle and set as 60° for a canopy with spherical leaf angle distribution; and θ is the solar zenith angle.

Diffuse and direct PAR were partitioned using the formula following Chen et al. (1999) with parameters calibrated using daily diffuse and total incoming radiation data measured at Nanjing, Shanghai, Ganzhou, and Nanchang in China, i.e.

$$PAR_{dif} = PAR \times (0.7527 + 3.8453R - 16.316R^2 + 18.962R^3 - 7.0802R^4) \quad (10)$$

where PAR_{dif} represents the diffuse PAR; PAR is the total incoming photosynthetically active radiation, and R is the sky clearness index and equals ($PAR/0.5S_0\cos\theta$); S_0 is the solar constant (1367 W m^{-2}). A constant 0.5 is used to convert incoming solar radiation into PAR (Weiss and Norman, 1985; Tsubo and Walker, 2005; Jacovides et al., 2007; Bosch et al., 2009).

The LAI_{sh} and LAI_{su} in equations 8 and 9 are the LAI of shaded and sunlit leaves and are computed as (Chen et al., 1999):

$$LAI_{su} = 2 \times \cos(\theta) \times \left(1 - \exp\left(-0.5 \times \Omega \times \frac{LAI}{\cos(\theta)}\right)\right) \quad (11)$$

$$LAI_{sh} = LAI - LAI_{su} \quad (12)$$

where Ω is the clumping index, which depends on land cover types, season and solar zenith angles, and so on. Since spatially distributed data for this parameter are lacking, Ω is set according to vegetation types (Table 2).

2.3. Calibrating the maximum light use efficiency parameter

Parameters ε_{max} in Eq. (3) and ε_{msu} and ε_{msh} in Eq. (7) were calibrated using measured GPP. These parameters were tuned in the prescribed ranges until the root mean square error (RMSE) of modeled daily GPP against measured daily GPP (GPP_{EC}) approached the minimum value. The ranges of ε_{max} at CBS, QYZ and DHS were set to 0–12 g C MJ^{-1}, 0–4 g C MJ^{-1} at YC, and 0–2 g C MJ^{-1} at HB and XLHT (Zhang et al., 2006b, 2008). The ranges of ε_{msh} and ε_{msu} were set as two times as much as and 50% of those of ε_{max}, respectively. In the calibration process, these parameters were tuned at a step of 0.1 g C MJ^{-1}.

2.4. Criteria for model validation

Three criteria were used here to evaluate model performance, including determination coefficient (R^2), root mean square error (RMSE), and the relative error (RE). They are calculated as:

$$R^2 = \left(\frac{\sum_{i=1}^{N} (GPP_{EC}(i) - \overline{GPP_{EC}})(GPP_{sim}(i) - \overline{GPP_{sim}})}{\sqrt{\sum_{i=1}^{N} (GPP_{EC}(i) - \overline{GPP_{EC}})^2} \sqrt{\sum_{i=1}^{N} (GPP_{sim}(i) - \overline{GPP_{sim}})^2}} \right)^2 \quad (13)$$

$$RMSE = \sqrt{\frac{1}{N} \sum_{i=1}^{N} (GPP_{sim}(i) - GPP_{EC}(i))^2} \quad (14)$$

$$RE = \frac{GPP_{sim} - GPP_{EC}}{GPP_{EC}} \times 100\% \quad (15)$$

where GPP_{sim} is the GPP either calculated using the MOD17 algorithm (GPP_{MOD}) or the TL-LUE model developed here (GPP_{TL}); GPP_{EC} is the tower-measured GPP; the over-bars represent the mean values; and N is the sample number.

In addition to the validation with tower-based GPP, the ability of the TL-LUE model to simulate GPP was compared with that of the MOD17 algorithm, the remote sensing driven process-based BEPS model (Chen et al., 1999), and the VI model developed by Wu et al. (2010). The BEPS model calculates GPP of entire canopy through the separation of sunlit and shaded leaves based on biophysical process. The VI model calculates GPP as the product of EVI and PAR.

3. Results and discussion

3.1. Calculated daily GPP

In the calibration years, GPP calculated using the MOD17 algorithm driven by the calibrated ε_{max}, the smoothed MODIS LAI and

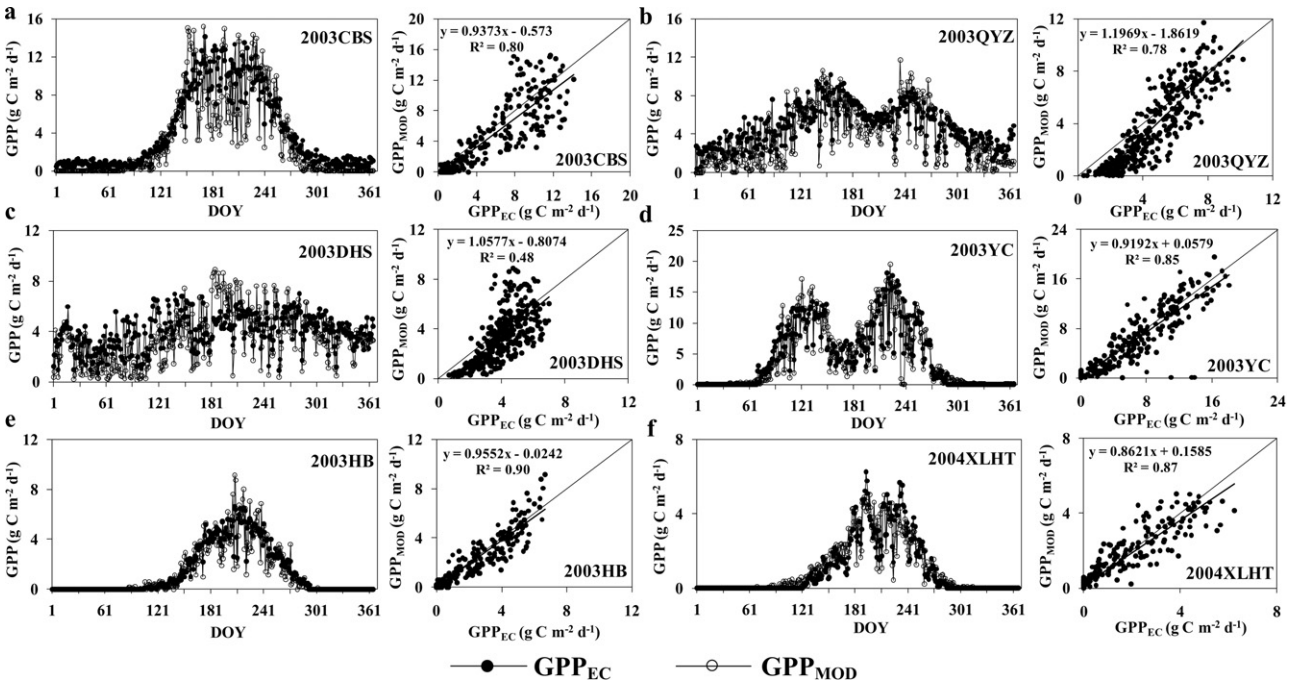

Fig. 2. Seasonal variations of daily measured GPP (GPP_{EC}) and GPP calculated using the MOD17 algorithm (GPP_{MOD}) in combination with calibrated ε_{max}, smoothed MODIS LAI and tower-based meteorological data in the calibration years at CBS (a), QYZ (b), DHS (c), YC (d), HB (e), and XLHT (f).

tower-measured meteorological data (GPP_{MOD}) show similar seasonal variations with GPP_{EC} (Fig. 2). At the CBS and QYZ forest sites and the HB and XLHT grassland sites, measured and calculated GPP exhibits distinguishable seasonality, e.g. low in spring and winter and high in summer and autumn, except that the seasonal variations of GPP at DHS are quite small. Crops of two rotations (winter wheat and summer maize) were cultivated at the YC site, resulting in two peaks of GPP in May and August, respectively, in which winter wheat and summer maize are at peaks of growth.

GPP_{MOD} has a good relationship with GPP_{EC}. The R^2 value of GPP_{MOD} against GPP_{EC} ranged from 0.48 (at DHS) to 0.90 (at HB). RMSE is in the range from 0.54 $g\,C\,m^{-2}\,d^{-1}$ (at XLHT) to 2.11 $g\,C\,m^{-2}\,d^{-1}$ (at CBS). The consistency between GPP_{MOD} and GPP_{EC} is better at grassland sites than at forest and cropland sites. Since ε_{max} was calibrated using measured daily GPP at the annual scale, it was actually the annual average of maximum LUE under different conditions of radiation and LAI. GPP calculated using ε_{max} calibrated in this way and the MOD17 algorithm is mostly lower

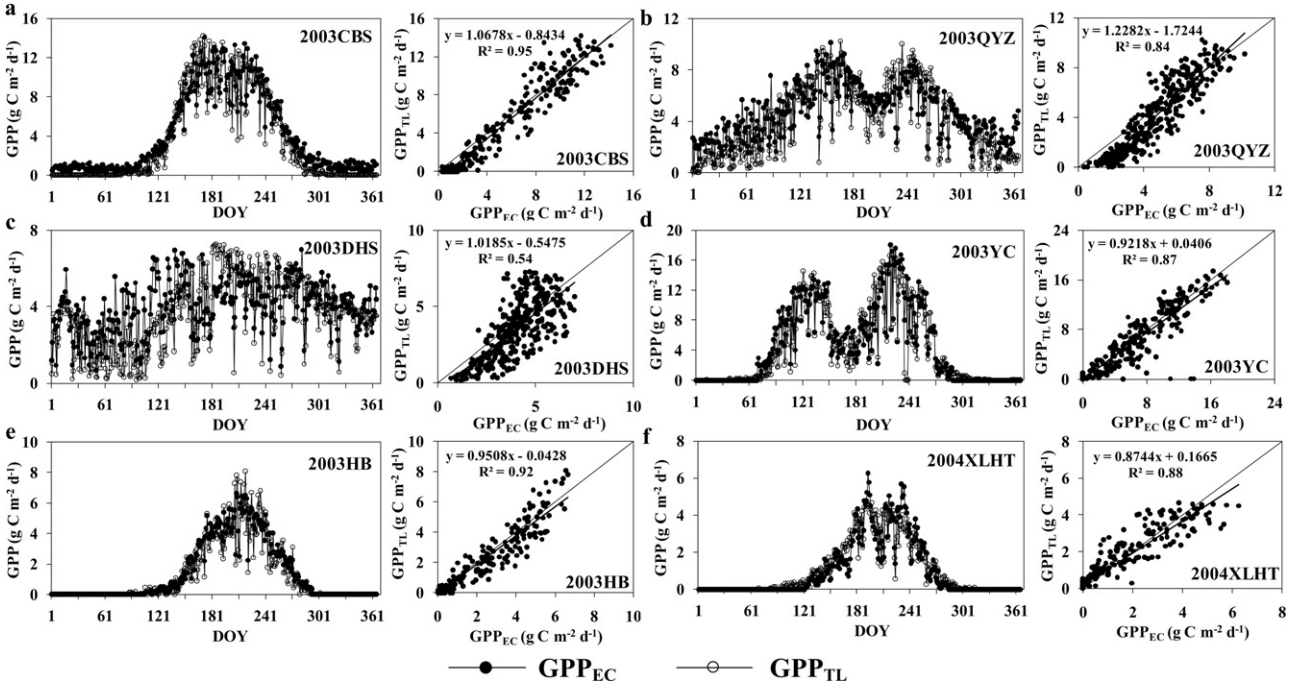

Fig. 3. Seasonal variations of daily measured GPP (GPP_{EC}) and GPP calculated using the TL-LUE model alone with calibrated ε_{msu} and ε_{msh}, smoothed MODIS LAI and tower-based meteorological data in the calibration years (GPP_{TL}) at CBS (a), QYZ (b), DHS (c), YC (d), HB (e), and XLHT (f).

than GPP_{EC} in overcast days with low total incoming PAR and higher in clear days with high total incoming PAR (Fig. 2) due to the fact that the MOD17 algorithm ignores the changes of LUE with sky conditions.

Fig. 3 exhibits the comparison of GPP_{EC} with GPP calculated using the TL-LUE model driven by the calibrated ε_{msu} and ε_{msh}, smoothed LAI, and tower-based meteorological data (GPP_{TL}) in the calibration years. At all sites, GPP_{TL} matched GPP_{EC} well. The R^2 values of GPP_{TL} against GPP_{EC} were in the range from 0.54 (at DHS) to 0.95 (at CBS). The RMSE value of GPP_{TL} was the lowest at XLHT in 2004 (0.48 g C m^{-2} d^{-1}) and the highest at YC in 2003 (1.83 g C m^{-2} d^{-1}). At all sites, GPP_{TL} has higher R^2 values and lower RMSE values than GPP_{MOD}, indicating that the TL-LUE model outperforms the MOD17 algorithm in calculating GPP at these 6 typical sites. The most significant improvement achieved by the TL-LUE model was at the CBS site, with R^2 increased from 0.80 to 0.95 and RMSE decreased from 2.11 to 1.22 g C m^{-2} d^{-1}, respectively.

Figs. 4 and 5 show the comparison of GPP_{EC} with GPP calculated using the MOD17 algorithm and TL-LUE model in conjunction with calibrated ε_{max}, ε_{msh}, ε_{msu}, smoothed LAI, and tower-based meteorological data in validation years, respectively. The TL-LUE model performs much better than the MOD17 algorithm at three forest sites, especially at CBS and QYZ. The R^2 values of GPP calculated using the MOD17 algorithm against measured GPP were 0.77 at CBS and 0.78 at QYZ, respectively. The corresponding values for GPP calculated using the TL-LUE model increase to 0.93 and 0.90 (Figs. 4 and 5). The improvement of TL-LUE over the MOD17 algorithm is marginal at HB and XLHT grassland sites because at these sites the shaded leaf contribution is small. In addition, the agreement between simulated GPP (GPP_{MOD} and GPP_{TL}) and measured GPP (GPP_{EC}) was poorer in the validation years than in calibration years at DHS, YC, XLHT, mainly due to the considerable differences of soil water content in the calibration and validations years and the exclusion of the effect of soil water content on GPP. Therefore, further efforts are need to develop an applicable and reliable method for describing the control of soil water content on GPP.

Fig. 6 shows the comparison of daily GPP calculated using the BEPS model (GPP_B) with GPP_{EC} in validation years. It shows that BEPS performs the best at CBS with a R^2 value of 0.90 and a RMSE value of 1.76 g C m^{-2} d^{-1}, followed by the HB site with a R^2 value of 0.86 and a RMSE value of 0.97 g C m^{-2} d^{-1}. However, GPP_B is obviously overestimated at DHS and seriously underestimated at XLHT. According to the R^2 and RMSE values of calculated GPP against GPP_{EC}, the TL-LUE model performs slightly better than the BEPS model at the CBS, DHS, and HB sites. It obviously outperforms the BEPS model at QYZ, YC, and XLHT sites, with R^2 increased by 0.14–0.20 and RMSE decreased by 0.16–0.96 g C m^{-2} d^{-1} (Figs. 5 and 6).

Table 3
Calibrated ε_{max}, ε_{msu} and ε_{msh} at the 6 sites.

Site	CBS	QYZ	DHS	YC	HB	XLHT
Year	2003	2003	2003	2003	2003	2004
ε_{max} (g C MJ^{-1})	2.216	1.508	0.859	2.904	1.804	0.904
ε_{msu} (g C MJ^{-1})	0.9	0.8	0.4	1.5	0.8	0.5
ε_{msh} (g C MJ^{-1})	4.3	2.8	1.5	5.3	3.5	2.3

In the validation years, R^2 values of GPP simulated using the VI model range from 0.37 (DHS) to 0.87 (HB) and RMSE is in the range from 0.80 g C m^{-2} d^{-1} (at XLHT) to 3.48 g C m^{-2} d^{-1} (at YC) (Fig. 7). The TL-LUE model performs better than the VI model at all sites, especially at the CBS, QYZ, YC sites. The R^2 values of GPP_{TL} against GPP_{EC} are 0.08 (at XLHT) to 0.34 (at CBS) higher than the corresponding values of GPP_{VI}. The RMSE values of GPP_{TL} are 0.12 g C m^{-2} d^{-1} (at XLHT) to 1.75 g C m^{-2} d^{-1} (at CBS) smaller than those of GPP_{VI}.

3.2. Calibrated maximum light use efficiency

Calibrated parameters ε_{max}, ε_{msu}, and ε_{msh} are shown in Table 3. At CBS, QYZ, YC, HB, and XLHT, calibrated ε_{max} is significantly higher than the default values used in the MOD17 algorithm (Tables 2 and 3). However, calibrated ε_{max} at DHS is lower than the default value. Calibrated ε_{max} varies significantly in different ecosystems. Calibrated ε_{max} of croplands is higher than those of grasslands and forests. For the same type of ecosystems, calibrated ε_{max} might differ considerably. For example, land cover types at the HB and XLHT sites are both grasslands, but calibrated ε_{max} is 1.804 g C MJ^{-1} at HB in 2003 and is 0.904 g C MJ^{-1} at XLHT in 2004, indicating the necessity of more detailed parameterization of ε_{max} in LUE models.

At all 6 sites, optimized ε_{msh} is 2.5–3.8 times larger than ε_{msu}, supporting the hypothesis that shaded leaves have higher LUE than sunlit leaves. Calibrated ε_{msu} ranges from 0.4 g C MJ^{-1} (at DHS)

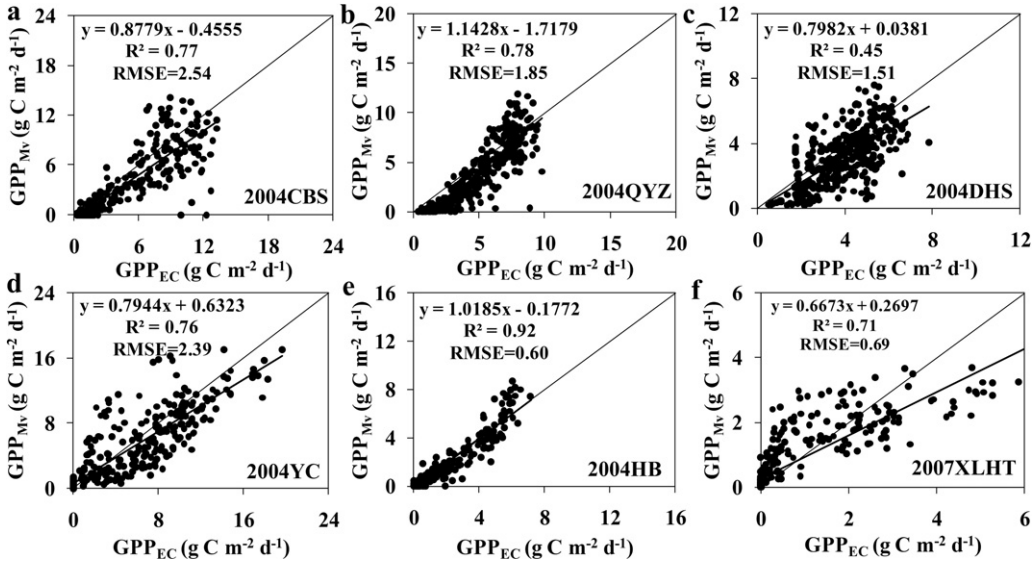

Fig. 4. Validation of daily GPP calculated using the MOD17 algorithm in conjunction with the calibrated ε_{max}, smoothed LAI, and tower-based meteorological data at CBS (a), QYZ (b), DHS (c), YC (d), HB (e) in 2004, and at XLHT (f) in 2007 (RMSE in unit of g C m^{-2} d^{-1}).

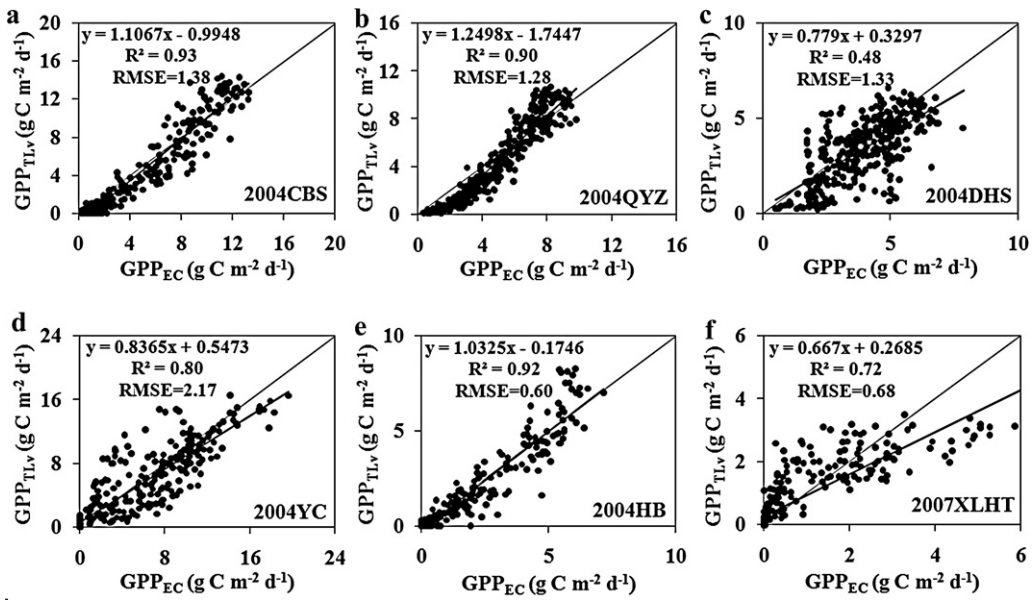

Fig. 5. Validation of GPP calculated using the TL-LUE model in conjunction with the calibrated ε_{msu} and ε_{msh}, smoother LAI, and tower-based meteorological data at CBS (a), QYZ (b), DHS (c), YC (d), HB (e) in 2004, and at XLHT (f) in 2007 (RMSE in unit of g C m^{-2} d^{-1}).

to 1.5 g C MJ^{-1} (at YC) while calibrated ε_{msh} is in the range from 1.5 g C MJ^{-1} (at DHS) to 5.3 g C MJ^{-1} (at YC). ε_{msu} and ε_{msh} of cropland at YC are higher than those of forests and grasslands. At all sites, calibrated ε_{msh} is about two times as much as the calibrated ε_{max} used in the MOD17 algorithm while calibrated ε_{msu} is about 45% to 59% lower than the calibrated ε_{max}.

3.3. The sensitivity of calculated daily GPP to sky clearness

The comparison of GPP calculated using the MOD17 algorithm with measured GPP shows that GPP is systematically underestimated under the conditions of low incoming radiation and overestimated under the conditions of high incoming radiation (Fig. 2). In order to investigate the degree, at which the errors of calculated daily GPP change with sky conditions, absolute differences between calculated and measured GPP were binned according to sky clearness index for the calibration years (Fig. 8). When R is below 0.5, GPP is systematically underestimated by the MOD17 algorithm. The underestimation of GPP becomes more serious with the decrease of R. When R is above 0.5, GPP is systematically overestimated. The overestimation of GPP by the MOD17 algorithm under the conditions of clear skies was also recently reported by Propastin et al. (2012).

The TL-LUE model greatly alleviates the sensitivity of calculated GPP to sky conditions (Fig. 8). The underestimation of GPP calculated by the TL-LUE model is smaller than that of GPP calculated by the MOD17 algorithm under the conditions of R smaller than 0.5. The TL-LUE model also has much smaller overestimation of GPP than the MOD17 algorithm when R is above 0.5. The smaller changes in the departure of GPP calculated by the TL-LUE model

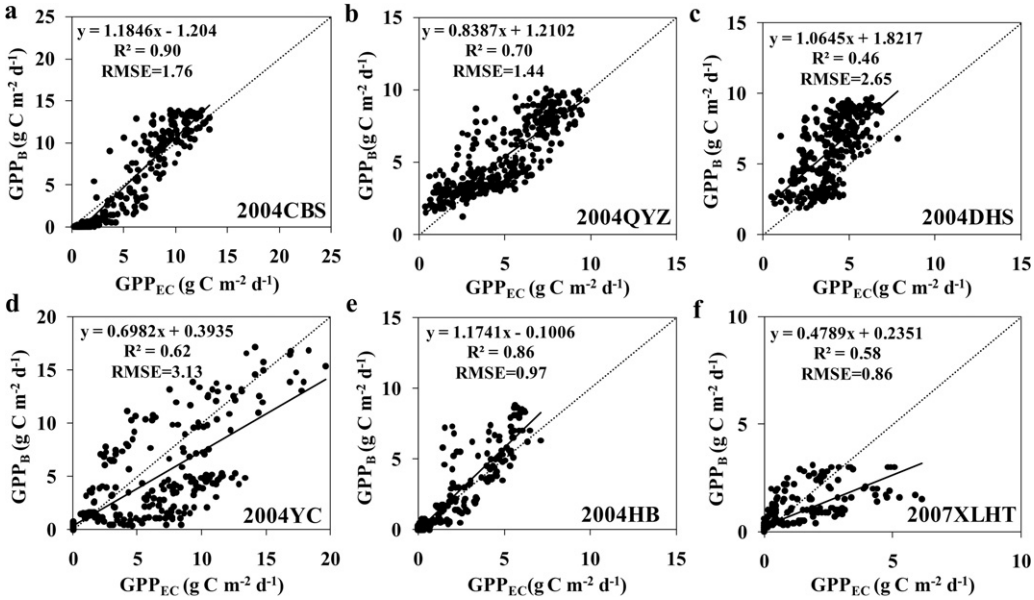

Fig. 6. Comparison of daily GPP calculated using the BEPS model (GPP_B) with measured GPP (GPP_{EC}) at CBS (a), QYZ (b), DHS (c), YC (d), HB (e) in 2004 and XLHT (f) in 2007 (RMSE in unit of g C m^{-2} d^{-1}).

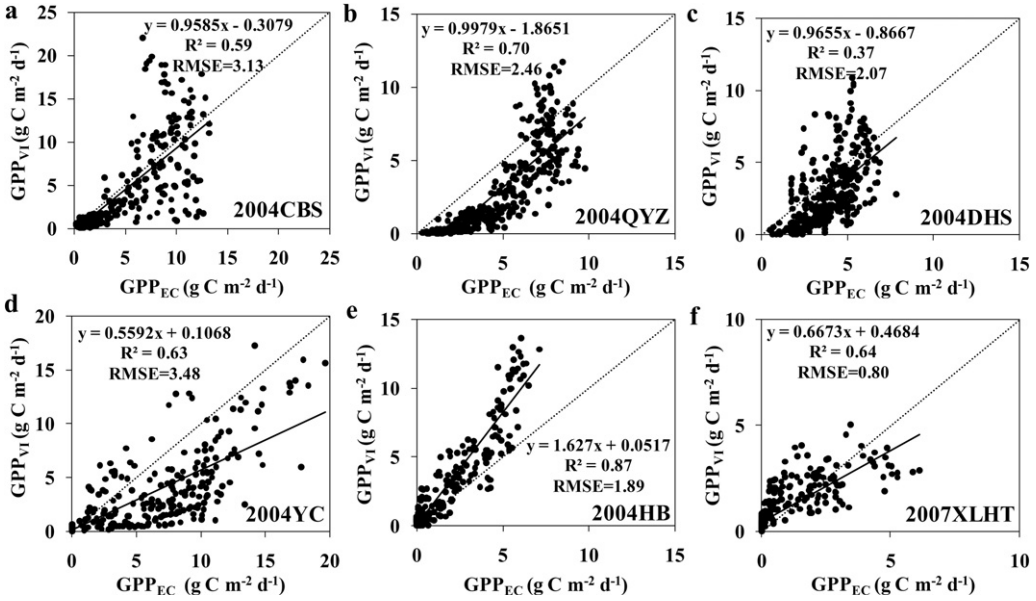

Fig. 7. Comparison of GPP calculated by the VI model (GPP_{VI}) with measured GPP (GPP_{EC}) and at CBS (a), QYZ (b), DHS (c), YC (d), HB (e) in 2004 and at XLHT (f) in 2007 (RMSE in unit of g C m^{-2} d^{-1}).

from measurements might be attributable to following reasons. When *R* is low, diffuse PAR accounts for a large fraction of incoming PAR. The ratio of APAR by shaded leaves to APAR of the entire canopy APAR increases. Since ε_{msh} is larger than ε_{msu} and ε_{max}, GPP_{TL} is larger than GPP_{MOD}. When *R* is high, direct PAR accounts for a large fraction of incident PAR and the fraction of diffuse PAR is low. APAR by sunlit leaves is the dominant fraction of APAR of the entire canopy. Because ε_{msu} is much lower than ε_{max}, GPP_{TL} is lower than GPP_{MOD}, resulting in less overestimation of GPP to some extent.

LUE is affected by a number of factors, including temperature, atmospheric humidity, total radiation, and fraction of diffuse radiation. Temperature and humidity are correlated with *R*, which determines the fraction of diffuse radiation (Zhang et al., 2011). Therefore, the change of mean LUE in different ranges of *R* was used as the indicator of LUE changing with meteorological conditions. Fig. 9 shows the changes of daily canopy light use efficiency (LUE_C = GPP/PAR) observed at towers and simulated using the MOD17 algorithm and the TL-LUE model in the growing seasons (May to September) of calibration and validation years. At all sites, observed LUE_C shows obviously decreasing trends with increasing sky clearness index *R*. In general, the TL-LUE model is also able to reproduce these trends. However, LUE_C simulated by the MOD17 algorithm does not decrease with the increase of *R* at the CBS, QYZ, and DHS forests sites. When *R* is above 0.35 (more direct radiation), the averages of observed and simulated LUE_C are similar. Simulated LUE_C is higher than the corresponding observed values at the DHS and YC sites when *R* is larger than 0.45. The overestimation of LUE_C simulated by the MOD17 algorithm is more serious. Under the conditions of cloudy skies with *R* smaller than 0.35 (more diffuse

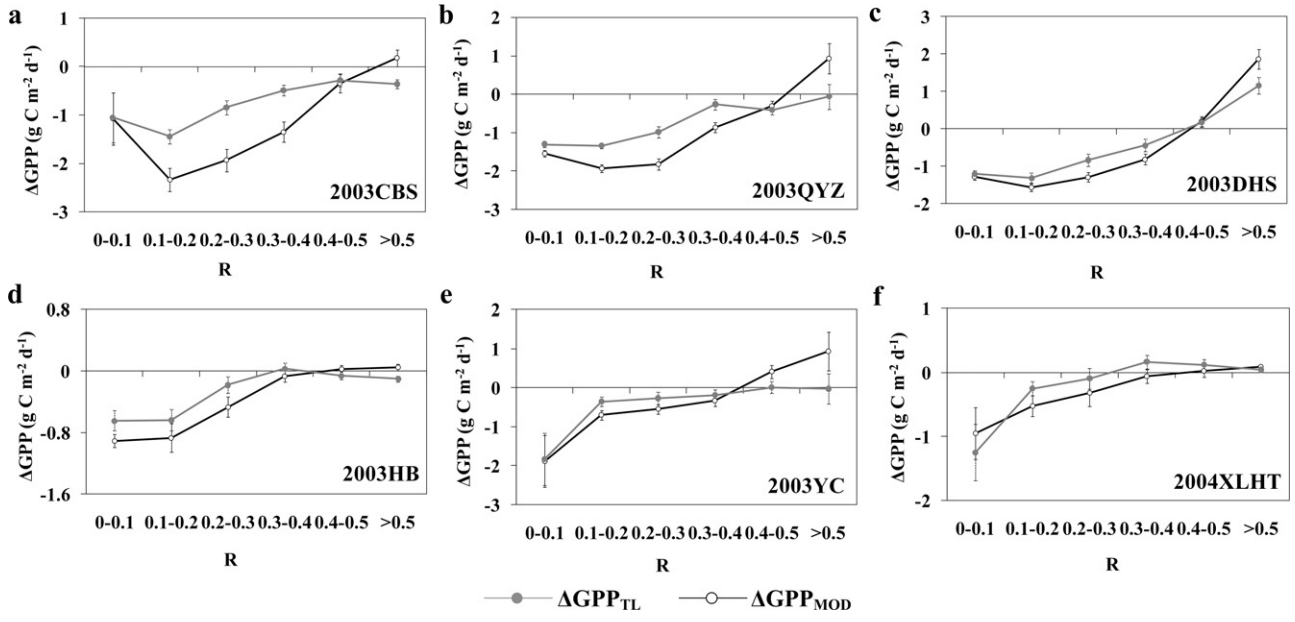

Fig. 8. Dependence of the average absolute errors of GPP estimated using calibrated parameters with sky clearness index R ($R = s_g/(s_0 \cos\theta)$) sites ($\Delta GPP_{MOD} = GPP_{MOD} - GPP_{EC}$, $\Delta GPP_{TL} = GPP_{TL} - GPP_{EC}$, negative values mean the underestimation of GPP by models, vice versa).

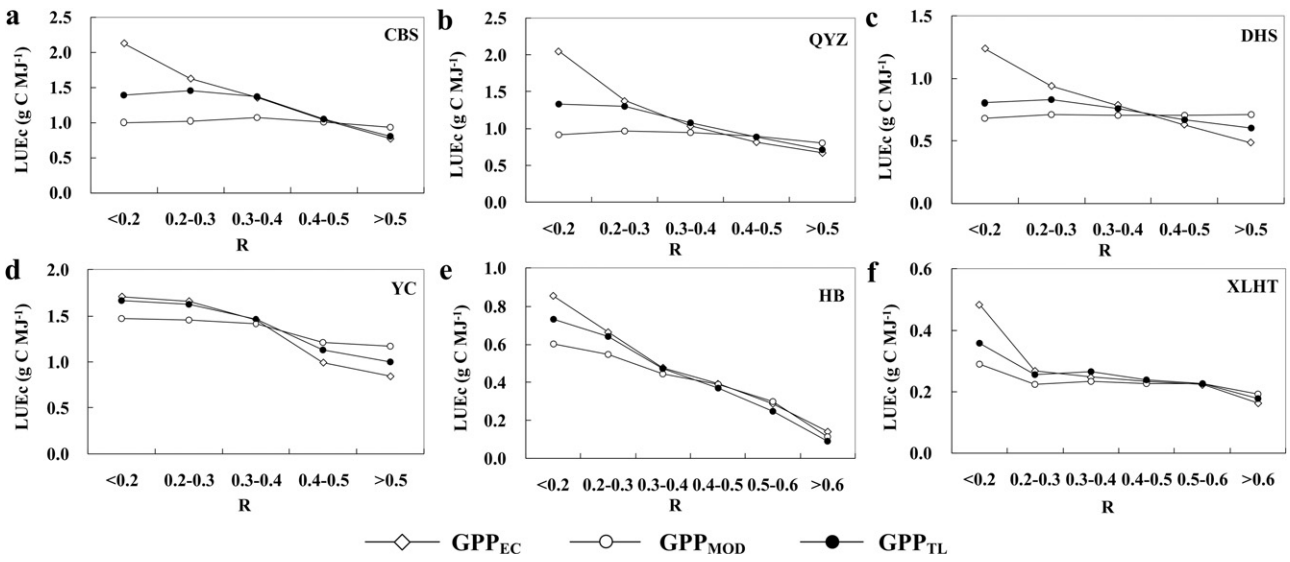

Fig. 9. Observed and modeled dependence of canopy light use efficiency (LUEc = GPP/PAR) on sky clearness index (R) averaged over 0.1 bins of R in the growing seasons (May to September) of the calibration and validation years.

radiation), the MOD17 algorithm and TL-LUE model tend to underestimate LUE_C. The underestimation by the MOD17 algorithm is more obvious.

The changes of observed and simulated LUE_C with R identified here indicates that big-leaf LUE models, such as the MOD17 algorithm, might be able to simulate average GPP over a longer time period through calibrating the parameter ε_{max}. Without the consideration of the effect of light quantity on GPP, it tends to underestimate GPP in days and regions with more cloudy and aerosol laden skies having lower total incoming radiation and higher fractions of diffuse radiation. The TL-LUE model developed here differentiates the LUE of sunlit and shaded leaves and the transfer of direct and diffuse radiation within the canopy, resulting in the better performance in calculating GPP and LUE_C than the MOD17 algorithm. Of course, this model currently treats the LUE of sunlit and shaded leaves as constants, leading to non-negligible underestimation of GPP and LUE_C under the conditions of low R values and high diffuse radiation fractions. In order to further improve

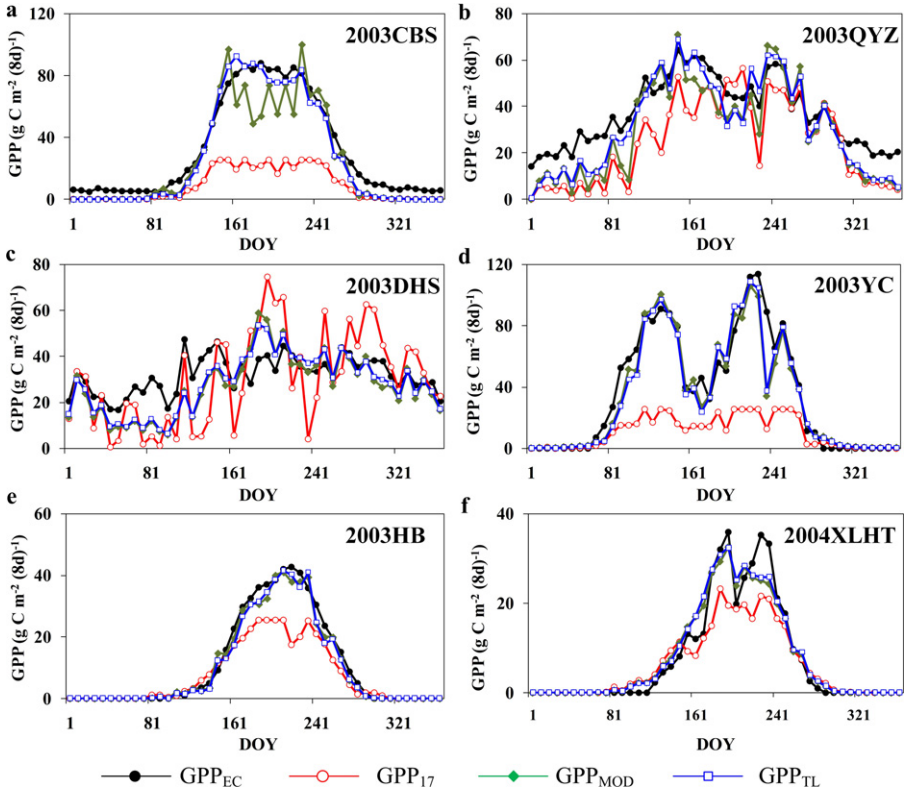

Fig. 10. Seasonal variations of 8-day GPP_{EC}, GPP_{17}, GPP_{MOD} and GPP_{TL} at CBS (a), QYZ (b), DHS (c), YC (d), and HB (e) in 2003 and at XLHT (f) in 2004 (GPP_{MOD} and GPP_{TL} are the GPP calculated with the MOD17 algorithm and the TL-LUE model driven by measured meteorological data, smoothed LAI and calibrated ε_{max}, ε_{msu} and ε_{msh}, respectively GPP_{17} is the MODIS GPP product).

Table 4
Statistics for the comparison of 8-day MODIS GPP product (GPP_{17}) and 8-day GPP calculated using the MOD17 algorithm (GPP_{MOD}) and the TL-LUE model (GPP_{TL}) with tower-measured GPP (GPP_{EC}) at the 6 study sites.

Site	Year	Annual average ($g C m^{-2} (8d)^{-1}$)				RE (%)			R^2			RMSE ($g C m^{-2} (8d)^{-1}$)		
		GPP_{EC}	GPP_{17}	GPP_{MOD}	GPP_{TL}	GPP_{17}	GPP_{MOD}	GPP_{TL}	GPP_{17}	GPP_{MOD}	GPP_{TL}	GPP_{17}	GPP_{MOD}	GPP_{TL}
CBS	2003	32.15	8.95	25.58	27.63	−72.2	−20.4	−14.0	0.91	0.88	0.98	31.87	12.67	6.83
	2004	31.84	9.35	24.32	27.32	−70.6	−23.6	−14.2	0.96	0.85	0.97	30.19	13.99	8.18
QYZ	2003	37.20	24.54	29.75	32.01	−34.0	−20.0	−14.0	0.72	0.87	0.93	15.90	11.15	8.83
	2004	38.44	19.87	30.26	34.16	−48.3	−21.3	−11.1	0.68	0.84	0.96	20.98	12.65	8.32
DHS	2003	31.75	29.82	27.18	27.99	−6.1	−14.4	−11.8	0.37	0.55	0.58	17.00	10.08	9.09
	2004	30.84	25.74	24.92	26.65	−16.5	−19.2	−13.6	0.19	0.66	0.67	13.57	8.66	7.44
YC	2003	36.10	10.80	33.64	33.60	−70.1	−6.8	−6.9	0.86	0.92	0.92	37.76	10.85	10.67
	2004	34.96	11.76	32.80	33.60	−66.4	−6.2	−3.9	0.72	0.80	0.83	37.00	16.21	14.92
HB	2003	10.87	7.45	10.19	10.00	−31.4	−6.2	−8.0	0.94	0.98	0.98	7.18	2.17	2.23
	2004	10.80	7.10	9.59	9.76	−34.2	−11.2	−9.6	0.93	0.97	0.97	7.11	2.83	2.88
XLHT	2004	7.74	6.18	7.93	8.09	−20.2	2.5	4.6	0.93	0.96	0.97	4.98	2.72	2.67
	2007	5.70	4.19	5.94	5.93	−26.5	4.3	4.1	0.66	0.82	0.81	6.60	4.25	4.24

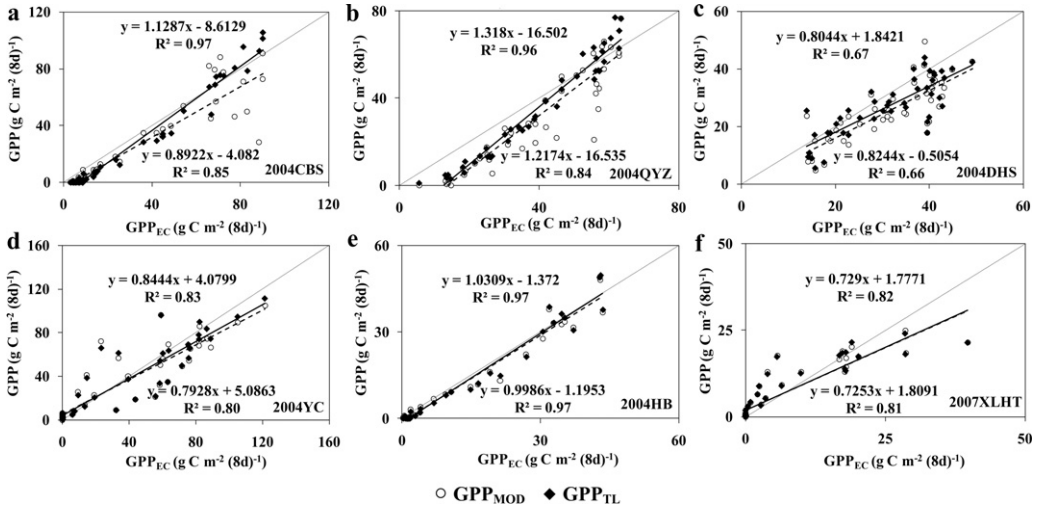

Fig. 11. Comparison of 8-day GPP_{EC}, GPP_{17}, GPP_{MOD} and GPP_{TL} at CBS (a), QYZ (b), DHS (c), YC (d), HB (e) in 2004 and at XLHT (f) in 2007 (GPP_{MOD} and GPP_{TL} are the GPP calculated with the MOD17 algorithm and the TL-LUE model driven by measured meteorological data, smoothed LAI and calibrated ε_{max}, ε_{msu} and ε_{msh}, respectively The linear regression equations in the top are for GPP_{TL} and those in the bottom are for GPP_{MOD}).

the calculation of GPP using LUE models, it is necessary to allow the LUE of sunlit and shaded leaves to vary with APAR.

3.4. Comparison of 8-day calculated GPP with measurements

Fig. 10 shows the time series of 8-day GPP_{EC}, MODIS GPP (GPP_{17}), GPP_{MOD} and GPP_{TL} at the 6 study sites in the calibration years (in 2003 at CBS, QYZ, DHS, YC, HB, and in 2004 at XLHT). GPP_{17} is systematically lower than measurements at all sites but the DHS site mainly due to the low default ε_{max} values used to produce the MOD17 product. With the calibration of ε_{max}, the systematic errors of GPP calculated using the MOD17 algorithm was removed (Fig. 9 and Table 4). The RE values of GPP_{17} range from −6.1% (at DHS) to −72.2% (at CBS) while the corresponding values of GPP_{MOD} are in the range from −20.4% (at CBS) to 2.5% (at XLHT). The R^2 values of GPP_{17} are in the range from 0.37 (at DHS) to 0.94 (at HB) and those of GPP_{MOD} vary from 0.55 (at DHS) and 0.98 (at HB). The RMSE values of GPP_{MOD} are significantly lower than those of GPP_{17}, especially at CBS and YC (Table 4). The closer agreement between GPP_{EC} and GPP_{MOD} indicates the applicability of this algorithm in calculating GPP for typical ecosystems in China.

Fig. 11 shows the comparison of 8-day GPP_{EC} with GPP_{MOD} and GPP_{TL} in the validation years at the 6 sites. In comparison with GPP_{MOD}, GPP_{TL} is much closer to GPP_{EC} with higher R^2 and lower RMSE values (Fig. 11 and Table 4). For instance, the R^2 value of GPP_{TL} against GPP_{EC} at CBS in 2004 is 0.97, much higher than the corresponding value of GPP_{MOD} which is 0.85.The RMSE value of GPP_{TL} is $8.18\,g C m^{-2} (8 d)^{-1}$, while that of GPP_{MOD} is $13.99\,g C m^{-2} (8d)^{-1}$.

In both calibration and validation years, 8-day GPP calculated using the TL-LUE model was obviously better than 8-day GPP_{17} and GPP_{MOD} at the three forest sites (Figs. 10 and 11 and Table 4), especially at CBS and QYZ. The improvement of GPP_{TL} over GPP_{MOD} mainly occurred during the growing season.

4. Conclusions

On the basis of the widely used MOD17 algorithm, a TL-LUE model is developed in this study. This new model considers the differences in the LUE of sunlit and shaded leaves and in the transfer of diffuse and direct radiation within the canopy in the calculation of GPP. GPP measured at 6 typical sites are used for model calibration and validation. The ability of the TL-LUE model to calculate GPP was also compared with that of the MOD17 algorithm. The main conclusions can be drawn as follows:

(1) The MODIS GPP product is systematically underestimated at the CBS, QYZ, YC, HB, and XLHT sites. Run with measured meteorological data, smoothed MODIS LAI, and calibrated ε_{max}, the MOD17 algorithm can reproduce GPP close to those derived from eddy-covariance measurements, indicating that the MOD17 algorithm is applicable to simulating GPP for

forest, cropland and grassland ecosystems in China when ε_{max} is properly determined.

(2) The TL-LUE model which separately calculates GPP for sunlit and shaded leaves outperforms the MOD17 algorithm in calculating daily and 8-day GPP, especially at forest sites. It even performs better than the remote sensing driven process-based BPES model at some sites and obviously better than the empirical VI model at all sites. This new model significantly reduces the systematic biases in simulated GPP under different sky conditions. The TL-LUE model developed here may be further improved by considering the variations of LUE within the sunlit and shaded leaf groups for high-LAI canopies.

(3) Calibrated ε_{max}, ε_{msu} and ε_{msh} exhibit considerable differences among different types of ecosystems. They also differ at different sites with the same vegetation types. LUE of shaded leaves (ε_{msh}) is considerably larger than that of sunlit leaves (ε_{msu}) due to the fact that shaded leaves are not light saturated.

The TL-LUE model is constructed on the basis of the MOD17 algorithm with the consideration of the differences in APAR and LUE between sunlit and shaded leaves. There are many factors that influence LUE. Same as the MOD17 algorithm, the TL-LUE model only includes the effects of minimum air temperature and vapor pressure deficit on LUE. The exclusion of the role of soil water content in regulating GPP and changes of LUE with APAR might have significantly limited the improvement of simulated GPP using the TL-LUE model. In addition, MODIS LAI plays an important role in the calculation of APAR. Its uncertainties could have significant impacts on the calibration of ε_{max}, ε_{msu}, ε_{msh}, and calculated GPP. This study ignores the uncertainties in MODIS LAI, which might be a contributor of the considerable departure of GPP calculated using the MOD 17 algorithm and the TL-LUE model from measurements at some sites, such as DHS and XLHT. This shortcoming should be taken into consideration seriously in the future research. In addition, the applicability and robustness of the TL-LUE model need validation at more sites in other regions.

Acknowledgements

This study is supported by the National Basic Research Program of China (2010CB0705002 and 2010CB833503),Doctoral Fund of Ministry of Education of China (20090091110034), the Chinese Academy of Sciences for Strategic Priority Research Program (No. XDA05050602) and the Priority Academic Program Development of Jiangsu Higher Education Institutions. We also greatly thank the ChinaFLUX for the provision of flux and meteorological data. The comments for two anonymous reviews are very constructive and help us considerably improve the quality of this manuscript.

References

Baldocchi, D.D., Falge, E., Gu, L., Olson, R., Hollinger, D.Y., Running, S.W., Anthoni, P., Bernhofer, Ch., Davis, K.J., Evans, R., Fuentes, J., Goldstein, A., Katul, G., Law, B.E., Lee, X., Malhi, Y., Meyers, T.P., Munger, J.W., Oechel, W.C., Paw, U.K.T., Pilegaard, K., Schmid, H.P., Valentini, R., Verma, S., Vesala, T., Wilson, K.B., Wofsy, S.C., 2001. FLUXNET: a new tool to study the temporal and spatial variability of ecosystem-scale carbon dioxide, water vapor, and energy flux densities. Bull. Am. Meteorol. Soc. 82, 2415–2434.

Bosch, J.L., López, G., Batlles, F.J., 2009. Global and direct photosynthetically active radiation parameterizations for clear-sky conditions. Agr. Forest Meteorol. 149, 146–158.

Chen, J.M., Deng, F., Chen, M., 2006. Locally adjusted cubic-spline capping for reconstructing seasonal trajectories of a satellite-derived surface parameter. IEEE Trans. Geosci. Remote Sens. 44, 2230–2238.

Chen, J.M., Liu, J., Cihlar, J., Guolden, M.L., 1999. Daily canopy photosynthesis model through temporal and spatial scaling for remote sensing applications. Ecol. Model. 124, 99–119.

De Pury, D.G.G., Farquhar, G.D., 1997. Simple scaling of photosynthesis from leaves to canopies without the errors of big-leaf models. Plant Cell Environ. 20, 537–557.

Field, C.B., Behrenfeld, M.J., Randerson, J.T., Falkowski, P., 1998. Primary production of the biosphere: integrating terrestrial and oceanic components. Science 281, 237–240.

Fu, Y.L., Yu, G.R., Wang, Y.F., Hao, Y.B., 2006a. Effect of water stress on ecosystem photosynthesis and respiration of *Leymus chinensis* steppe in Inner Mongolia. Sci. China Earth Sci. 49 (Suppl. 2), 196–206.

Fu, Y.L., Yu, G.R., Sun, X.M., Li, Y.N., Wen, X.F., Zhang, L.M., Li, Z.Q., Zhao, L., Hao, Y.B., 2006b. Depression of net ecosystem CO_2 exchange in semi-arid Leymus chinensis steppe and alpine shrub. Agr. Forest Meteorol. 137, 234–244.

Gao, Z.Q., Liu, J.Y., 2008. Comparison research of net primary productivity in China. Chin. Sci. Bull. 53, 317–326.

Grant, I.F., Prata, A.J., Cechet, R.P., 2000. The impact of the diurnal variation of albedo on the remote sensing of the daily mean albedo of grassland. J. Clim. Appl. Meteorol. 39, 231–244.

Gu, L.H., Baldocchi, D.D., Verma, S.B., Black, T.A., Vesala, T., Falge, E.M., Dowty, P.R., 2002. Advantages of diffuse radiation for terrestrial ecosystem productivity. J. Geophys. Res. 107, 1–23.

Gu, L.H., Baldocchi, D.D., Wofsy, S., Munger, J.M., Michalsky, J.J., Urnamski, S.P., Bolden, T.A., 2003. Response of a deciduous forest to the Mount Pinatubo eruption: enhanced photosynthesis. Science 299, 2035–2038.

Heinsch, F.A., Zhao, M.S., Running, S.W., Kimball, J.S., Nemani, R.R., Davis, K.J., Bolstad, P.V., Cook, B.D., Desai, A.R., Ricciuto, D.M., Law, B.E., Oechel, W.C., Kwon, H.J., Luo, H., Wofsy, S.C., Dunn, A.L., Munger, J.W., Baldocchi, D.D., Xu, L., Hollinger, D.Y., Richardson, A.D., Stoy, P.C., Siqueira, M.B.S., Monson, R.k., Burns, S.P., Flanagan, L.B., 2006. Evaluation of remote sensing based terrestrial productivity from MODIS using regional tower eddy flux network observations. IEEE Trans. Geosci. Remote Sens. 44 (7), 1908–1925.

Hill, M.J., Senarath, U., Lee, A., Melanie, Z., Joanne, M.N., Richard, J.W., Tim, R.M., 2006. Assessment of the MODIS LAI product for Australian ecosystems. Remote Sens. Environ. 101, 495–518.

Jacovides, C.P., Tymvios, F.S., Assimakopoulos, V.D., Kaltsounides, N.A., 2007. The dependence of global and diffuse PAR radiation components on sky conditions at Athens, Greece. Agr. Forest Meteorol. 143, 277–287.

Jarvis, P.G., Leverenz, J.W., 1983. Productivity of temperate deciduous and evergreen forests. In: Lange, O.L. (Ed.), Ecosystem Processes: Mineral Cycling, Productivity, and Man's Influence. Springer-Verlag, New York, pp. 233–280.

Li, J., Yu, Q., Sun, X.M., Tong, X.J., Ren, C.Y., Wang, J., Liu, E.M., Zhu, Z.L., Yu, G.R., 2006. Carbon exchange and its environmental regulation mechanisms in North China plain ecosystem. Sci. China Earth Sci. 49 (Suppl. 2), 226–240.

Li, Z.Q., 2006. Multi-scale analysis and scale changing of productivity of terrestrial ecosystem. Ph.D. Thesis. Beijing: Graduate University of Chinese Academy of Sciences (in Chinese with English abstract).

Lieth, H., 1973. Primary production: terrestrial ecosystem. Hum. Ecol. 1 (4), 303–332.

Liu, Y.B., Ju, W.M., Zhu, G.L., Chen, J.M., Xing, B.L., Zhu, J.F., Zhou, Y.L., 2011. Retrieval of leaf area index for different grasslands in Inner Mongolia prairie using remote sensing data. Acta Ecol. Sin. 31, 5159–5170 (in Chinese with English abstract).

Lloyd, J., Taylor, J.A., 1994. On the temperature dependence of soil respiration. Funct. Ecol. 8, 315–323.

Mercado, L.M., Bellouin, N., Sitch, S., Boucher, O., Huntingford, C., Wild, M., Cox, P.M., 2009. Impact of changes in diffuse radiation on the global land carbon sink. Nature 458, 1014–1018.

Metz, B., Davidson, O., Coninck, H.D., Loos, M., Meyer, L., 2006. A special report of the intergovernmental panel on climate change. Intergovernmental Panel on Climate Change. Cambridge University Press, Cambridge.

Misson, L., Lunden, M., McKay, M., Goldstein, A.H., 2005. Atmospheric aerosol light scattering and surface wetness influence the diurnal pattern of net ecosystem exchange in a semi-arid ponderosa pine plantation. Agr. Forest Meteorol. 129, 69–83.

Monteith, J.L., 1972. Solar radiation and productivity in tropical ecosystems. J. Appl. Ecol. 9, 747–766.

Nightingale, J.M., Coops, N.C., Waring, R.H., Hargrove, W.W., 2007. Comparison of MODIS gross primary production estimates for forests across the U.S.A. with those generated by a simple process model, 3-PGS. Remote Sens. Environ. 109, 500–509.

Niyogi, D., Chang, H.I., Saxena, V.K., Holt, T., Alapaty, K., Booker, F., Chen, F., Davis, K.J., Holben, B., Matsui, T., Meyers, T., Oechel, W.C., Pielke Sr., R.A., Wells, R., Wilson, K., Xue, Y.K., 2004. Direct observations of the effects of aerosol loading on net ecosystem CO_2 exchanges over different landscapes. Geophys. Res. Lett. 31, L20506.

Norman, J.M., 1993. Scaling processed between leaf and canopy levels. In: Ehleringer, J.R., Field, C.B. (Eds.), Scaling Physiological Processes: Leaf to Globe. Academic Press, San Diego, pp. 41–76.

Oliphant, A.J., Dragoni, D., Deng, B., Grimmond, C.S.B., Schmid, H.-P., Scott, S.L., 2011. The role of sky conditions on gross primary production in a mixed deciduous forest. Agr. Forest Meteorol. 151, 781–791.

Piao, S.L., Fang, J.Y., Zhou, L.M., Zhu, B., Tan, K., Tao, S., 2005. Changes in vegetation net primary productivity from 1982 to 1999 in China. Global Biogeochem. Cycles 19, GB2027.

Potter, C.S., Randerson, J.T., Field, C.B., Matson, P.A., Vitousek, P.M., Mooney, H.A., Klooster, S.A., 1993. Terrestrial ecosystem production: a process model based on global satellite and surface data. Global Biogeochem. Cycles 7, 811–841.

Propastin, P., Ibrom, A., Knohl, A., Erasmi, S., 2012. Effects of canopy photosynthesis saturation of gross primary productivity form MODIS data in a tropical forest. Remote Sens. Environ. 121, 252–260.

Roderick, M.L., Farquhar, G.D., Berry, S.L., Noble, B.I.R., 2001. On the direct effect of clouds and atmospheric particles on the productivity and structure of vegetation. Oecologia 129, 21–30.

Running, S.W., Thornton, P.E., Nemani, R., Glassy, J.M., 2000. Global terrestrial gross and net primary productivity from the Earth Observing system. In: Sala, O., Jackson, R., Mooney, H. (Eds.), Methods in Ecosystem Science. Springer-Verlag, New York, pp. 44–55.

Running, S.W., Nemani, R.R., Heinsch, F.A., Zhao, M.S., Reeves, M., Hashimoto, H., 2004. A continuous satellite-drived measure of global terrestrial primary production. BioScience 54, 547–560.

Singarayer, J.S., Ridgwell, A., Irvine, P., 2009. Assessing the benefits of crop albedo bio-geoengineering. Environ. Res. Lett. 4, 045110.

Sun, J.S., Zhou, G.S., 2010. Review of advances in measurements and effects of diffuse radiation on terrestrial ecosystem productivity. Chin. J. Plant Ecol. 34, 452–461 (in Chinese with English abstract).

Tang, S., Chen, J.M., Zhu, Q., Li, X., Chen, M., Sun, R., Zhou, Y., Deng, F., Xie, D., 2007. An LAI inversion algorithm based on directional reflectance kernels. J. Environ. Manage. 85, 638–648.

Tsubo, M., Walker, S., 2005. Relationships between photosynthetically active radiation and clearness index at Bloemfontein, South Africa. Theor. Appl. Climatol. 80, 17–25.

Turner, D.P., Ritts, W.D., Cohen, W.B., Gower, S.T., Running, S.W., Wofsy, S.C., Urbanski, S., Dunn, A.L., Munger, J.W., 2003. Scaling gross primary production (GPP) over boreal and deciduous forest landscaped in support of MODIS GPP product validation. Remote Sens. Environ. 88, 256–270.

Urban, O., Janous, D., Acosta, M., Czerný, R., Marková, I., Navrátil, M., Pavelka, M., Pokorný, R., šprtová, M., Zhang, R., špunda, V., Grace, J., Marek, M.V., 2007. Ecophysiological controls over the net ecosystem exchange of mountain spruce stand. Comparison of the response in direct vs. diffuse solar radiation. Global Change Biol. 13, 157–168.

Wang, S., Chen, J.M., Ju, W.M., Feng, X.F., Chen, M., Chen, P., Yu, G., 2007. Carbon sinks and sources in China's forests during 1901–2001. J. Environ. Manage. 85, 524–537.

Wang, Y.J., Woodcock, C.E., Buermann, W., Stenberg, P., Viopio, P., Smolander, H., Häme, T., Tian, Y., Hu, J.N., Knyazikhin, Y., Myneni, R.B., 2004. Evaluation of the MODIS LAI algorithm at a coniferous forest site in Finland. Remote Sens. Environ. 91, 114–127.

Wang, Y.P., Lenuing, R., 1998. A two-leaf model for canopy conductance, photosynthesis and partitioning of available energy I: model description and comparison with multi-layered model. Agr. Forest Meteorol. 91, 89–111.

Weiss, A., Norman, J.M., 1985. Partitioning solar radiation into direct and diffuse, visible and near-infrared components. Agr. Forest Meteorol. 34, 205–213.

Wu, C.Y., Niu, Z., Gao, S., 2010. Gross primary production estimation from MODIS data with vegetation index and photosynthetically active radiation in maize. J. Geophys. Res. 115, D12127.

Xiao, X.M., Hollinger, D., Aber, J., Goltz, M., Davidson, E.A., Zhang, Q.Y., Moore III, B., 2004a. Satellite-based modeling of gross primary production in an evergreen needle leaf forest. Remote Sens. Environ. 89, 519–534.

Xiao, X.M., Zhang, Q.Y., Braswell, B., Urbanski, S., Boles, S., Wofsy, S., Moore III, B., Ojima, D., 2004b. Modeling gross primary production of temperate deciduous broadleaf forest using satellite images and climate data. Remote Sens. Environ. 91, 256–270.

Yang, F.H., Ichii, K., White, M.A., Hashimoto, H., Michaelis, A.R., Votava, P., Zhu, A.X., Huete, A., Running, S.W., Nemani, R.R., 2007. Developing a continental-scale measure of gross primary production by combining MODIS and AmeriFlux data through Support Vector Machine approach. Remote Sens. Environ. 110, 109–122.

Yu, G.R., Wen, X.F., Sun, X.M., Tanner, B.D., Lee, X.H., Chen, J.Y., 2006. Overview of ChinaFLUX and evaluation of its eddy covariance measurement. Agr. Forest Meteorol. 137, 125–137.

Yu, G.R., Song, X., Wang, Q.F., Liu, Y.F., Guan, D.X., Yan, J.H., Sun, X.M., Zhang, L.M., Wen, X.F., 2008. Water-use efficiency of forest ecosystems in eastern China and its relations to climatic variables. New Phytolog. 177, 927–937.

Yuan, W.P., Liu, S.G., Zhou, G.S., Zhou, G.Y., Tieszen, L.L., Baldocchi, D.D., Bernhofer, C., Gholz, H., Goldstein, A.H., Goulden, M.L., Hollinger, D.Y., Hu, Y.M., Law, B.E., Stoy, P.C., Vesala, T., Wofsy, S.C., 2007. Deriving a light use efficiency model from eddy covariance flux data for predicting daily gross primary production across biomes. Agr. Forest Meteorol. 143, 189–207.

Zhang, L.M., Yu, G.R., Sun, X.M., Wen, X.F., Song, X., Liu, Y.F., Guan, D.X., Yan, J.H., Zhang, Y.P., 2006a. Seasonal variation of carbon exchange of typical forest ecosystems along the eastern forest transect in China. Sci. China Earth Sci. 49 (Suppl. 2), 47–62.

Zhang, L.M., Yu, G.R., Sun, X.M., Wen, X.F., Ren, C.Y., Fu, Y.L., Li, Q.K., Li, Z.Q., Liu, Y.F., Guan, D.X., Yan, J.H., 2006b. Seasonal variations of ecosystem apparent quantum yield (α) and maximum photosynthesis rate (P_{max}) of different forest ecosystems in China. Agr. Forest Meteorol. 17, 176–187.

Zhang, M., Yu, G.R., Zhuang, J., Gentry, R., Fu, Y.L., Sun, X.M., Zhang, L.M., Wen, X.F., Han, S.J., Yan, J.H., Zhang, Y.P., Wang, Y.F., Li, Y.N., 2011. Effects of cloudiness changes on net ecosystem exchange, light use efficiency, and water use efficiency in typical ecosystems of China. Agr. Forest Meteorol. 151, 803–816.

Zhang, Y.Q., Yu, Q., Jiang, J., Tang, Y.H., 2008. Calibration of Terra/MODIS gross primary production over an irrigated cropland on the North China Plain and an alpine meadow on the Tibetan Plateau. Global Change Biol. 14, 757–767.

Zhao, M.S., Heinsch, F.A., Nemani, R.R., Running, S.W., 2005. Improvements of the MODIS terrestrial gross and net primary production global data set. Remote Sens. Environ. 95, 164–176.

Zhao, M.S., Running, S.W., Nemani, R.R., 2006. Sensitivity of MODerate Resolution Imaging Spectroradiometer (MODIS) terrestrial primary production to the accuracy of meteorological reanalyzes. J. Geophys. Res. 111, 1002–1015.